The thin descending limb of the loop of Henle originates from proximal tubule cells during mouse kidney development

Eunah Chung,[1,2] Fariba Nosrati,[1,2] Mike Adam,[3] Andrew Potter,[3] Mohammed Sayed,[4] Benjamin D. Humphreys,[5,6] Hee-Woong Lim,[4,7] Yueh-Chiang Hu,[3,7] S. Steve Potter,[3,7] and Joo-Seop Park[1,2,*]

[1]Division of Nephrology and Hypertension, Northwestern University Feinberg School of Medicine, Chicago, IL, USA

[2]Feinberg Cardiovascular and Renal Research Institute, Chicago, IL, USA

[3]Division of Developmental Biology, Cincinnati Children's Hospital Medical Center, Cincinnati, OH, USA

[4]Division of Biomedical Informatics, Cincinnati Children's Hospital Medical Center, Cincinnati, OH, USA

[5]Division of Nephrology, Department of Medicine, Washington University, St. Louis, MO, USA

[6]Department of Developmental Biology, Washington University, St. Louis, MO, USA

[7]Department of Pediatrics, University of Cincinnati, Cincinnati, OH, USA

The word count for the abstract: 270

The word count for the text: 2737

The number of figures: 4

[*]Corresponding author:

Joo-Seop Park

Division of Nephrology and Hypertension

Feinberg Cardiovascular and Renal Research Institute

Northwestern University Feinberg School of Medicine

303 E. Superior St., SQBRC 8-406, Chicago, IL 60611

Email: jooseop.park@northwestern.edu

Key Points

- Reference single cell RNA-seq dataset of the developing mouse kidney was assembled and used to identify the thin descending limb of the loop of Henle.
- Lineage analysis of proximal tubules in the mouse kidney shows that proximal tubule cells give rise to the thin descending limb of the loop of Henle.
- Deletion of Hnf4a disrupts the expression of *Aqp1* in the thin descending limb of the loop of Henle, highlighting a developmental link between proximal tubules and the loop of Henle.

Abstract

Background

The thin descending limb (DTL) of the loop of Henle is crucial for urine concentration, as it facilitates passive water reabsorption. Despite its importance, little is known about how DTL cells form during kidney development. Single-cell RNA sequencing (scRNA-seq) studies have not definitively identified DTL cells in the developing mouse kidney.

Methods

We assembled a large scRNA-seq dataset by integrating multiple datasets of non-mutant developing mouse kidneys to identify developing DTL cells. To test whether DTL cells originate from proximal tubule (PT) cells, we generated a PT-specific Cre line, *Slc34a1eGFPCre*, and conducted lineage tracing of PT cells. Additionally, given that the transcription factor Hnf4a directly binds to the *Aqp1* gene, we examined whether the loss of Hnf4a affects *Aqp1* expression in DTL cells.

Results

From our scRNA-seq dataset, we identified a small cluster of cells distinct from both the proximal tubule and the thick ascending limb of the loop of Henle. Those cells exhibited high expression of DTL marker genes, including *Aqp1* and *Bst1*. Notably, a subset of PT cells also expressed DTL marker genes, suggesting that PT cells may give rise to DTL cells. Using lineage tracing with the *Slc34a1eGFPCre* line, we found that DTL cells were positive for the Rosa26 reporter, confirming that DTL cells are descendants of PT cells. Furthermore, the loss of Hnf4a, a transcription factor essential for mature PT cell formation, disrupted proper *Aqp1* expression in DTL cells, providing additional evidence of a developmental link between PT cells and DTL cells.

Conclusion

Our findings shed new light on the developmental origin of DTL cells and highlight the importance of Hnf4a in regulating their formation.

Introduction

Mesenchymal nephron progenitor cells (mNPs) have the potential to differentiate into any cell type within the nephron.[1] During development, the mesenchymal-to-epithelial transition (MET) of mNPs leads to the formation of the renal vesicle (RV), which develops into the S-shaped body (SSB).[2,3] Although it is known that Wnt,[4-6] Fgf,[7,8] and Notch[9,10] signaling pathways play critical roles in the initial differentiation, it remains poorly understood how the SSB progresses into a fully developed nephron. This is, at least in part, due to the fact that nephron formation is not synchronized in the mammalian kidney. New nephrons form in waves, largely occurring alongside the branching of the ureteric epithelium. This asynchronous development makes it challenging to study the development of the nephron in a stepwise manner.

Single-cell RNA sequencing (scRNA-seq) offers a powerful tool to help overcome this obstacle with its capability to address cellular heterogeneity.[11] In this study, we leveraged scRNA-seq to investigate how different nephron segments are formed. Our analysis of the mouse kidney reveals that the thin descending limb (DTL) of the loop of Henle (LOH) emerges from proximal tubule (PT) cells, providing new insights into the developmental origin of the DTL. Additionally, the comprehensive scRNA-seq dataset and the PT-specific Cre line presented here will serve as valuable resources and tools for kidney research.

Methods

Mice

Slc34a1eGFPCre was generated by modifying the previously reported *Slc34a1eGFPCreERT2*[12] with CRISPR.[13] The guide RNA target sequence (GGCGATCTCGAGCCATCTGC) was selected according to the on- and off-target scores from the web tool CRISPOR (http://crispor.tefor.net).[14] The chemically modified single-guide RNA (sgRNA) was purchased from IDT. To form ribonucleoprotein complex (RNP), sgRNA was mixed with Cas9 protein (IDT) in Opti-MEM (ThermoFisher) and incubated at 37°C for 10 min. The donor oligo (Ultramer from IDT) with the intended mutations to introduce a stop codon and asymmetrical homologous arm

design was added to the RNP.[15] The final concentrations are 60 ng/μl of sgRNA, 80 ng/μl of Cas9 protein, and 500 ng/μl of donor oligo. The zygotes carrying *Slc34a1eGFPCreERT2* from superovulated female mice were electroporated with 7 μl of the RNP/donor mix on ice using a Genome Editor electroporator (BEX; 30V, 1ms width, and 5 pulses with 1s interval). Two minutes after electroporation, zygotes were moved into 500 μl cold M2 medium (Sigma), warmed up to room temperature, and then transferred into the oviductal ampulla of pseudopregnant CD-1 females. Pups were genotyped by PCR, EcoRI digest, and Sanger sequencing. Other mouse alleles used in this study have been previously reported: *Rosa26 LacZ* (JAX:003474),[16] *Hnf4a flox*,[17] *Osr2IresCre* (JAX:009388),[18] *Rosa26 NuTrap* (JAX:029899),[19] and *Six2TGC* (JAX:009606).[1,5] Animals were housed in a controlled environment with a 12-h light/12-h dark cycle, with free access to water and a standard chow diet. All experiments were performed in accordance with animal care guidelines and the protocols were approved by the Institutional Animal Care and Use Committee of Cincinnati Children's Hospital Medical Center or Northwestern University. We adhere to the NIH Guide for the Care and Use of Laboratory Animals.

scRNA-seq

Dissociation was performed using psychrophilic proteases.[20] Briefly, tissue was digested in the buffer containing 10 mg/ml *Bacillus Licheniformis* enzyme (Sigma, P5380) for 20 min, with trituration and vigorous shaking. The digest mixture was then filtered using a 30 μM filter (Miltenyi). The flow-through was centrifuged at 300g for 5 min at 4°C. Supernatant was removed, and the pellet was resuspended in 1 ml phosphate-buffered saline (PBS) containing 10% FBS, followed by filtration using a 20 μM filter (pluriSelect), and centrifuging the flow-through at 300 g for 5 min at 4°C. The pellet was resuspended in 0.4-1 ml ice-cold 10% FBS/PBS. After the cell suspension was analyzed using a hemocytometer with trypan blue, 9600 cells were loaded into the 10X Chromium instrument for each sample, and Gel Beads in Emulsion (GEMs) were generated. 10X Genomics 3' v3.1 chemistry was used, using the protocol provided by 10X Genomics, with 14 cycles for cDNA amplification. Single cell libraries were sequenced using the NovaSeq 6000.

scRNA-seq data analysis

Fastq files were processed through the CellRanger pipeline v6.1.2[21] using 10X Genomics' mm10 reference genome, with the setting include introns set to True. Background reads were removed using decontX from the celda package[22] using the filtered barcodes as the cells to keep and the remaining cells in the raw barcode matrix as the background. Doublets were minimized using DoubletFinder.[23] The R v4.1.1 library Seurat v4.9[24] was used for cell type clustering and marker gene identification. Cells expressing >500 genes were retained for downstream analysis. Each sample was normalized SCTransform (v2), using the glmGamPoi method and the number of RNA molecules per cell were regressed out. The effect of cycling cells was regressed out using cell cycle phase scoring. Samples were integrated with the top 3000 common anchor genes to minimize sample to sample variation. Cell clusters were determined by the Louvain algorithm using a resolution of 0.5. UMAP dimension reduction was done using the first thirty principal components. Marker genes for each cell type were calculated using the Wilcoxon Rank Sum test returning only genes that are present in a minimum of 25% of the analyzed cluster. Manual curation of the resulting data was performed by removing cell clusters that were considered junk, clustering only by ribosomal genes, or high mitochondrial gene content. Stromal cells were further subclustered using Seurat's FindClusters function. To estimate the number of stromal subtypes, clustering was repeated multiple times, each using a different resolution value (ranges from 0.02 to 1, step = 0.02). Then, the resolution value corresponding to the most frequent number of clusters was picked (resolution = 0.36). Marker genes of stromal subtypes were predicted using the same criteria mentioned above with the exception of including only genes whose expression in the analyzed cluster is at least 0.5 log fold-change higher compared to their average expression in other clusters.

Immunofluorescence Staining

Kidneys were fixed in PBS containing 4% paraformaldehyde for 15 min, incubated overnight in 10% sucrose/PBS at 4°C, and embedded in OCT (Fisher Scientific). Cryosections (8-10μm) were incubated overnight with primary antibodies in PBS containing 5% heat-inactivated sheep serum and 0.1% Triton X-100. Primary antibodies used in this study are listed in Supplemental Table 1. Fluorophore-labeled secondary antibodies were used for indirect visualization of the target. Images were taken with a Nikon Ti-2 inverted widefield microscope equipped with an Orca Fusion camera and Lumencor Spectra III light source.

Results

Realizing that scRNA-seq datasets with limited cell numbers often fail to show the presence of rare cell types, we assembled a reference scRNA-seq dataset (67,438 cells) by combining seven scRNA-seq datasets of non-mutant mouse kidneys at embryonic day 18.5 (E18.5) or postnatal day 0 (P0) (Figure 1A, Supplemental Figure 1, Supplemental Table 2).[25] At this stage, active nephrogenesis still occurs while nephron tubule cells with segmental identities are already formed. Therefore, this dataset captures all stages of nephrogenesis, including undifferentiated mNPs, epithelial nephron progenitors (eNPs) present in nascent nephron structures such as RV and SSB, along with mature nephron segments. Batch correction was successful as the same cell types from each sample clustered together (Supplemental Figure 2).

FeaturePlots in Figure 1B show a brief timeline of mNPs developing into distinct nephron segments. mNPs express *Cited1*[26,27] and *Six2*,[1,28] genes that are downregulated when mNPs undergo MET to become eNPs. During differentiation, *Wnt4*[5,6,29] and *Osr2*[18] are sequentially activated. According to previous lineage analyses, *Wnt4Cre* targets all nephron segments[10] while *Osr2Cre* targets all nephron segments except for the distal tubule (DT).[30] eNPs eventually develop into the four major cell types of the nephron: podocytes, PT, LOH, and DT.

Most scRNA-seq studies of mouse kidneys to date have used *Slc12a1* as a marker for LOH,[31,32] which consists of the thin descending limb (DTL), thin ascending limb, and thick ascending limb (TAL). However, while *Slc12a1* effectively marks TAL, it does not capture the entire LOH (Supplemental Figure 3). To identify DTL cells in our scRNA-seq dataset, we analyzed genes specifically expressed in DTL using previously reported bulk RNA-seq data generated from microdissected nephron segments of adult mouse kidneys (GSE150338).[33] Consistent with a previous report,[34] we found that *Bst1* and *Aqp1* were preferentially expressed in DTL (Supplemental Table 3). FeaturePlots revealed that both genes were strongly expressed in a small cluster adjacent to the PT cluster (black arrows in Figure 2A). Notably, this small cluster with high *Bst1* and *Aqp1*

expression showed little or no expression of the PT marker *Slc34a1* or the TAL marker *Slc12a1* (Figure 1B), distinguishing it from PT or TAL cells. These observations suggest that this cluster likely represents DTL cells.

Interestingly, both *Bst1* and *Aqp1* were also detectable at the upper edge of the PT cluster (Figure 2A). The PT segment can be divided into three subsegments: the convoluted S1 and S2 segments and the straight S3 segment. In the developing mouse kidney, the S1 segment appeared distinct from the S2/S3 segments (Figure 2B). Genes specific to S1, such as *Slc5a2*, were expressed in the lower part of the PT cluster, while S2/S3-specific genes, such as *Slc5a8* and *Kap*, were expressed in the upper part.[33] Notably, *Ihh*, which has been shown to be expressed in the straight PT tubules (S3 segment) of the developing kidney,[35] exhibited strong expression at the upper edge of the PT cluster (Figure 2B). This expression pattern was intriguing, as both DTL marker genes, *Bst1* and *Aqp1*, appeared to be expressed in the S3 segment of PT (Figure 2A). To validate this finding, we performed immunostaining. As shown in Figure 2C, Hnf4a+ straight tubules (S3 segment) of the developing mouse kidney were also positive for Aqp1. Since *Aqp1* is continuously expressed in DTL cells, this result raises the intriguing possibility that PT cells in the S3 segment may give rise to DTL cells.

In order to test if DTL cells originate from PT cells, we generated a new PT-specific Cre line. The expression of *Slc34a1* is highly specific for PT cells (Figure 1B).[33] We converted the tamoxifen-inducible *Slc34a1eGFPCreERT2*[12] to a constitutively active Cre (*Slc34a1eGFPCre*) by inserting a stop codon immediately after the Cre coding sequence (Supplemental Figure 4). With this new Cre line, we performed lineage tracing of PT cells. In the adult mouse kidney, convoluted PT cells (S1 and S2 segments) exhibited strong LTL staining, whereas straight PT tubules (S3 segment) showed weaker LTL staining (Figure 3A). All PT cells across these segments expressed *Hnf4a*. When the *Rosa26-Sun1* reporter was activated by *Slc34a1eGFPCre*, the reporter was expressed in most Hnf4a+ cells in the S1 and S2 segments, as well as in a subset of Hnf4a+ cells in the S3 segment (Figure 3A). This indicates that *Slc34a1Cre* targets all three PT segments with minor mosaicism in the S3 segment. Additionally, the reporter was activated in Hnf4a- cells

located in the medulla. These cells were identified as DTL cells based on their positive expression of *Aqp1* and lack of *Slc12a1* (Figure 3B). This result indicates that DTL cells are descendants of PT cells.

Our finding that PT cells give rise to DTL cells led us to investigate the potential role of Hnf4a in DTL formation. Previously, we showed that Hnf4a is required for the formation of mature PT cells.[36,37] Moreover, our chromatin immunoprecipitation analysis of Hnf4a in the developing mouse kidneys showed that Hnf4a directly binds to the promoter of *Aqp1*, a gene highly expressed in DTL (Supplemental Figure 5).[37] In the mouse kidney lacking Hnf4a, *Aqp1* expression in the mouse kidney was reduced by 50% (GSE144772).[37] The remaining *Aqp1* expression in *Hnf4a* mutant kidneys likely originated from endothelial cells (Figure 2A). These observations suggest that Hnf4a may play a regulatory role in *Aqp1* expression in DTL.

Nephron segments are spatially organized along the cortico-medullary axis of the kidney. LOH is located in the medulla and papilla of the kidney while the other nephron segments are strictly located at the cortex. This is achieved, at least in part, by elongation of LOH through the boundary of the cortex and medulla (Supplemental Figure 3).[38] To examine LOH formation in the *Hnf4a* mutant and control kidneys, we examined the cells in the nephron lineage located in the medulla of the kidney by performing the lineage tracing with *Osr2Cre*, which targets all nephron segments except for DT.[30] We found that both control and mutant kidneys formed nephron tubules in the medulla of the kidney and that both kidneys formed Slc12a1+ TAL (Figure 4A). This result suggests that the absence of Hnf4a does not affect the elongation of LOH nor the formation of TAL.

In the developing mouse kidney, *Aqp1* is expressed in both DTL cells and a subset of endothelial cells (Figure 2A). To distinguish between these two *Aqp1*+ cell populations, we performed co-staining for *Aqp1* along with the *Rosa26 LacZ* lineage tracer activated by *Osr2Cre* and the endothelial marker *Pecam1* (Figure 4B). In the control kidney, all *Aqp1*+ straight tubules overlapped with either β-galactosidase or *Pecam1*. Specifically, β-galactosidase+ *Aqp1*+ cells represented DTL cells, while *Pecam1*+ *Aqp1*+ cells represented endothelial cells. In the *Hnf4a* mutant kidney, however, most of the *Aqp1*+ long tubules were also positive for *Pecam1*, indicating endothelial cells. While β-galactosidase+ *Aqp1*+ cells were still present in the mutant kidney, *Aqp1* expression

was restricted to a short segment of tubules (Figure 4B). We found that DTL cells in the *Hnf4a* mutant kidney show defective expression of *Aqp1*, highlighting the critical role of Hnf4a in nephron segmentation beyond PT cells.

Discussion

In this study, we provide new insights into the developmental origin of DTL cells in LOH. By analyzing a large integrated scRNA-seq dataset, we identified a distinct cluster of cells with high expression of DTL marker genes, namely *Aqp1* and *Bst1*. Our lineage tracing experiments using the PT-specific *Slc34a1eGFPCre* line further confirmed that DTL cells are descendants of PT cells. Additionally, we demonstrated that the transcription factor Hnf4a, which plays a critical role in PT maturation,[36,37] is also essential for proper *Aqp1* expression in DTL cells. These findings collectively highlight a developmental connection between PT and DTL cells and reveal an important regulatory role for Hnf4a in DTL cell differentiation.

The assembly of a large scRNA-seq dataset allowed us to identify DTL cells, a rare cell type whose presence has been elusive in previous single-cell studies of the developing mouse kidney. It is unclear why the presence of DTL cells is harder to detect in scRNA-seq data than that of TAL cells. One possible explanation is that the dissociation procedure used to generate single-cell suspensions introduces biases in cellular composition. Some cell types, such as DTL cells, may be more sensitive to enzymatic or mechanical dissociation, resulting in loss or damage during sample preparation. As a result, the cell diversity observed in scRNA-seq data may not accurately represent the true *in vivo* cellular composition.

Aqp1 and Slc12a1 not only serve as markers for DTL and TAL, respectively, but also play critical physiological roles in LOH.[39,40] Slc12a1 (also known as NKCC2) in TAL actively reabsorbs sodium, potassium, and chloride ions from the filtrate traveling the lumen of the nephron, contributing to the hyperosmotic gradient in the medulla of the kidney.[41] Aqp1 in DTL allows passive water reabsorption driven by the osmotic gradient established by TAL.[42] This coordinated expression of transporters and channels along the LOH segments

establishes and maintains the medullary osmotic gradient, enabling the kidney to concentrate urine via a mechanism known as countercurrent multiplication.[43,44]

The observation that *Aqp1*, a DTL marker gene, is also expressed in the S3 segment of PT cells suggested a developmental connection between PT and DTL cells. Our lineage tracing analysis using the PT-specific *Slc34a1eGFPCre* provided strong evidence that DTL cells originate from PT cells. Consistent with this, we found that Hnf4a plays a critical role in regulating *Aqp1* expression in DTL cells, despite the fact that DTL cells exhibit little to no expression of *Hnf4a*. Interestingly, while *Aqp1* is weakly expressed in convoluted PT cells of the S1/S2 segments, the more robust *Aqp1* expression seen in DTL cells appears to require more than the direct binding of Hnf4a to the *Aqp1* gene. This raises the possibility that Hnf4a may function as a pioneering factor, as observed in other cell types,[45,46] by making the *Aqp1* gene accessible to another, yet unidentified, regulatory factor.

In summary, our study establishes a previously unrecognized developmental link between PT cells and DTL cells, advancing our understanding of nephron segmentation during kidney development. While our findings provide important insights, further studies are needed to uncover the molecular mechanisms driving the transition from PT cells to DTL cells with the downregulation of Hnf4a.

Disclosures

The authors have nothing to disclose.

Funding

This work was supported by National Institutes of Health, National Institute of Diabetes and Digestive and Kidney Diseases grants DK125577, DK131052, DK127634, DK120847 (to J.-S. Park), and DK120842 (to S.S. Potter).

Author Contributions

Conceptualization: Eunah Chung, Joo-Seop Park

Data curation: Mike Adam, Joo-Seop Park

Formal analysis: Mike Adam, Mohammed Sayed, Hee-Woong Lim

Funding acquisition: S. Steve Potter, Joo-Seop Park

Investigation: Eunah Chung, Fariba Nosrati, Joo-Seop Park

Methodology: Eunah Chung, Fariba Nosrati, Andrew Potter, Benjamin D. Humphreys, Yueh-Chiang Hu

Project administration: Joo-Seop Park

Resources: Benjamin D. Humphreys, S. Steve Potter, Joo-Seop Park

Software: Mike Adam, Mohammed Sayed, Hee-Woong Lim

Validation: Eunah Chung, Fariba Nosrati, Joo-Seop Park

Visualization: Eunah Chung, Mike Adam, Joo-Seop Park

Writing - original draft: Eunah Chung, Joo-Seop Park

Writing - review & editing: Eunah Chung, Mike Adam, Joo-Seop Park

Data Sharing Statement

The scRNA-seq data generated in this study were deposited at the Gene Expression Omnibus (GEO) under accession numbers GSE202882 and GSE275601.

References

1. Kobayashi A, Valerius MT, Mugford JW, et al. Six2 defines and regulates a multipotent self-renewing nephron progenitor population throughout mammalian kidney development. Research Support, N.I.H., Extramural
Research Support, Non-U.S. Gov't. *Cell Stem Cell*. Aug 7 2008;3(2):169-81. doi:10.1016/j.stem.2008.05.020

2. McMahon AP. Development of the Mammalian Kidney. *Curr Top Dev Biol*. 2016;117:31-64. doi:10.1016/bs.ctdb.2015.10.010

3. Schnell J, Achieng M, Lindström NO. Principles of human and mouse nephron development. *Nature Reviews Nephrology*. 2022;doi:10.1038/s41581-022-00598-5

4. Carroll TJ, Park JS, Hayashi S, Majumdar A, McMahon AP. Wnt9b plays a central role in the regulation of mesenchymal to epithelial transitions underlying organogenesis of the mammalian urogenital system. *Dev Cell*. Aug 2005;9(2):283-92. doi:10.1016/j.devcel.2005.05.016

5. Park JS, Valerius MT, McMahon AP. Wnt/beta-catenin signaling regulates nephron induction during mouse kidney development. Research Support, N.I.H., Extramural
Research Support, U.S. Gov't, P.H.S. *Development*. Jul 2007;134(13):2533-9. doi:10.1242/dev.006155

6. Park JS, Ma W, O'Brien LL, et al. Six2 and Wnt regulate self-renewal and commitment of nephron progenitors through shared gene regulatory networks. *Dev Cell*. Sep 11 2012;23(3):637-51. doi:10.1016/j.devcel.2012.07.008

7. Grieshammer U, Cebrian C, Ilagan R, Meyers E, Herzlinger D, Martin GR. FGF8 is required for cell survival at distinct stages of nephrogenesis and for regulation of gene expression in nascent nephrons. Research Support, N.I.H., Extramural
Research Support, Non-U.S. Gov't
Research Support, U.S. Gov't, P.H.S. *Development*. Sep 2005;132(17):3847-57. doi:10.1242/dev.01944

8. Perantoni AO, Timofeeva O, Naillat F, et al. Inactivation of FGF8 in early mesoderm reveals an essential role in kidney development. *Development*. Sep 2005;132(17):3859-71. doi:10.1242/dev.01945

9. Chung E, Deacon P, Marable S, Shin J, Park JS. Notch signaling promotes nephrogenesis by downregulating Six2. *Development*. Nov 1 2016;143(21):3907-3913. doi:10.1242/dev.143503

10. Chung E, Deacon P, Park JS. Notch is required for the formation of all nephron segments and primes nephron progenitors for differentiation. *Development*. Dec 15 2017;144(24):4530-4539. doi:10.1242/dev.156661

11. Park J, Liu CL, Kim J, Susztak K. Understanding the kidney one cell at a time. *Kidney Int*. Oct 2019;96(4):862-870. doi:10.1016/j.kint.2019.03.035

12. Kusaba T, Lalli M, Kramann R, Kobayashi A, Humphreys BD. Differentiated kidney epithelial cells repair injured proximal tubule. *Proc Natl Acad Sci U S A*. Jan 28 2014;111(4):1527-32. doi:10.1073/pnas.1310653110

13. Barrangou R, Doudna JA. Applications of CRISPR technologies in research and beyond. *Nat Biotechnol*. 2016;34(9):933-941. doi:10.1038/nbt.3659

14. Haeussler M, Schonig K, Eckert H, et al. Evaluation of off-target and on-target scoring algorithms and integration into the guide RNA selection tool CRISPOR. *Genome Biol*. Jul 5 2016;17(1):148. doi:10.1186/s13059-016-1012-2

15. Paix A, Folkmann A, Goldman DH, et al. Precision genome editing using synthesis-dependent repair of Cas9-induced DNA breaks. *Proc Natl Acad Sci U S A*. Dec 12 2017;114(50):E10745-E10754. doi:10.1073/pnas.1711979114

16. Soriano P. Generalized lacZ expression with the ROSA26 Cre reporter strain. *Nat Genet*. Jan 1999;21(1):70-1. doi:10.1038/5007

17. Parviz F, Li J, Kaestner KH, Duncan SA. Generation of a conditionally null allele of hnf4alpha. *Genesis*. Feb 2002;32(2):130-3.

18. Lan Y, Wang Q, Ovitt CE, Jiang R. A unique mouse strain expressing Cre recombinase for tissue-specific analysis of gene function in palate and kidney development. Research Support, N.I.H., Extramural. *Genesis*. Oct 2007;45(10):618-24. doi:10.1002/dvg.20334

19. Roh HC, Tsai LT, Lyubetskaya A, Tenen D, Kumari M, Rosen ED. Simultaneous Transcriptional and Epigenomic Profiling from Specific Cell Types within Heterogeneous Tissues In Vivo. *Cell reports*. Jan 24 2017;18(4):1048-1061. doi:10.1016/j.celrep.2016.12.087

20. Adam M, Potter AS, Potter SS. Psychrophilic proteases dramatically reduce single-cell RNA-seq artifacts: a molecular atlas of kidney development. *Development*. Oct 1 2017;144(19):3625-3632. doi:10.1242/dev.151142

21. Zheng GX, Terry JM, Belgrader P, et al. Massively parallel digital transcriptional profiling of single cells. *Nat Commun*. Jan 16 2017;8:14049. doi:10.1038/ncomms14049

22. Campbell J YS, Wang Z, Corbett S, Koga Y. celda: CEllular Latent Dirichlet Allocation. R package version 1.22.0. 2024;

23. McGinnis CS, Murrow LM, Gartner ZJ. DoubletFinder: Doublet Detection in Single-Cell RNA Sequencing Data Using Artificial Nearest Neighbors. *Cell Syst*. Apr 24 2019;8(4):329-337 e4. doi:10.1016/j.cels.2019.03.003

24. Hao Y, Hao S, Andersen-Nissen E, et al. Integrated analysis of multimodal single-cell data. *Cell*. Jun 24 2021;184(13):3573-3587 e29. doi:10.1016/j.cell.2021.04.048

25. Rudman-Melnick V, Adam M, Stowers K, et al. Single-cell sequencing dissects the transcriptional identity of activated fibroblasts and identifies novel persistent distal tubular injury patterns in kidney fibrosis. *Sci Rep*. Jan 3 2024;14(1):439. doi:10.1038/s41598-023-50195-0

26. Boyle S, Shioda T, Perantoni AO, de Caestecker M. Cited1 and Cited2 are differentially expressed in the developing kidney but are not required for nephrogenesis. *Dev Dyn*. Aug 2007;236(8):2321-30. doi:10.1002/dvdy.21242

27. Boyle S, Misfeldt A, Chandler KJ, et al. Fate mapping using Cited1-CreERT2 mice demonstrates that the cap mesenchyme contains self-renewing progenitor cells and gives rise exclusively to nephronic epithelia. Research Support, N.I.H., Extramural. *Developmental biology*. Jan 1 2008;313(1):234-45. doi:10.1016/j.ydbio.2007.10.014

28. Self M, Lagutin OV, Bowling B, et al. Six2 is required for suppression of nephrogenesis and progenitor renewal in the developing kidney. Research Support, N.I.H., Extramural

Research Support, Non-U.S. Gov't. *Embo J*. Nov 1 2006;25(21):5214-28. doi:10.1038/sj.emboj.7601381

29. Stark K, Vainio S, Vassileva G, McMahon AP. Epithelial transformation of metanephric mesenchyme in the developing kidney regulated by Wnt-4. Research Support, Non-U.S. Gov't

Research Support, U.S. Gov't, P.H.S. *Nature*. Dec 15 1994;372(6507):679-83. doi:10.1038/372679a0

30. Deacon P, Concodora CW, Chung E, Park J-S. β-catenin regulates the formation of multiple nephron segments in the mouse kidney. *Scientific Reports*. Nov 4 2019;9(1):15915. doi:10.1038/s41598-019-52255-w

31. Miao Z, Balzer MS, Ma Z, et al. Single cell regulatory landscape of the mouse kidney highlights cellular differentiation programs and disease targets. *Nat Commun*. Apr 15 2021;12(1):2277. doi:10.1038/s41467-021-22266-1

32. Muto Y, Wilson PC, Ledru N, et al. Single cell transcriptional and chromatin accessibility profiling redefine cellular heterogeneity in the adult human kidney. *Nat Commun*. Apr 13 2021;12(1):2190. doi:10.1038/s41467-021-22368-w

33. Chen L, Chou CL, Knepper MA. A Comprehensive Map of mRNAs and Their Isoforms across All 14 Renal Tubule Segments of Mouse. *J Am Soc Nephrol*. Apr 2021;32(4):897-912. doi:10.1681/ASN.2020101406

34. Ransick A, Lindstrom NO, Liu J, et al. Single-Cell Profiling Reveals Sex, Lineage, and Regional Diversity in the Mouse Kidney. *Dev Cell*. Nov 4 2019;51(3):399-413 e7. doi:10.1016/j.devcel.2019.10.005

35. Fabian SL, Penchev RR, St-Jacques B, et al. Hedgehog-Gli pathway activation during kidney fibrosis. Research Support, N.I.H., Extramural

Research Support, Non-U.S. Gov't. *Am J Pathol*. Apr 2012;180(4):1441-53. doi:10.1016/j.ajpath.2011.12.039

36. Marable SS, Chung E, Adam M, Potter SS, Park JS. Hnf4a deletion in the mouse kidney phenocopies Fanconi renotubular syndrome. *JCI Insight*. Jul 25 2018;3(14)doi:10.1172/jci.insight.97497

37. Marable SS, Chung E, Park JS. Hnf4a Is Required for the Development of Cdh6-Expressing Progenitors into Proximal Tubules in the Mouse Kidney. *J Am Soc Nephrol*. Aug 6 2020;doi:10.1681/ASN.2020020184

38. Nakai S, Sugitani Y, Sato H, et al. Crucial roles of Brn1 in distal tubule formation and function in mouse kidney. *Development*. Oct 2003;130(19):4751-9. doi:10.1242/dev.00666

39. Mount DB. Thick ascending limb of the loop of Henle. *Clin J Am Soc Nephrol*. Nov 7 2014;9(11):1974-86. doi:10.2215/CJN.04480413

40. Zacchia M, Capolongo G, Rinaldi L, Capasso G. The importance of the thick ascending limb of Henle's loop in renal physiology and pathophysiology. *Int J Nephrol Renovasc Dis*. 2018;11:81-92. doi:10.2147/IJNRD.S154000

41. Takahashi N, Chernavvsky DR, Gomez RA, Igarashi P, Gitelman HJ, Smithies O. Uncompensated polyuria in a mouse model of Bartter's syndrome. *Proc Natl Acad Sci U S A*. May 9 2000;97(10):5434-9. doi:10.1073/pnas.090091297

42. Ma T, Yang B, Gillespie A, Carlson EJ, Epstein CJ, Verkman AS. Severely impaired urinary concentrating ability in transgenic mice lacking aquaporin-1 water channels. *J Biol Chem*. Feb 20 1998;273(8):4296-9. doi:10.1074/jbc.273.8.4296

43. Imai M, Taniguchi J, Tabei K. Function of thin loops of Henle. *Kidney Int*. Feb 1987;31(2):565-79. doi:10.1038/ki.1987.37

44. Sands JM, Kokko JP. Countercurrent system. *Kidney Int*. Oct 1990;38(4):695-9. doi:10.1038/ki.1990.261

45. Hansen JL, Cohen BA. A quantitative metric of pioneer activity reveals that HNF4A has stronger in vivo pioneer activity than FOXA1. *Genome Biol*. Oct 17 2022;23(1):221. doi:10.1186/s13059-022-02792-x

46. Hansen JL, Loell KJ, Cohen BA. A test of the pioneer factor hypothesis using ectopic liver gene activation. *eLife*. Jan 5 2022;11doi:10.7554/eLife.73358

Supplemental Material

Figure Legends

Figure 1. Reference scRNA-seq dataset of the mouse kidney at E18.5 and P0 (A) UMAP plot showing 24 clusters of cells identified in the developing mouse kidney (B) FeaturePlots showing a brief timeline of nephrogenesis. mNPs express *Cited1* and *Six2*, while eNPs express *Wnt4* and *Osr2*. The eNPs develop into four major cell types: podocytes, PT, LOH, and DT.

Figure 2. Identification of DTL cells from scRNA-seq dataset (A) FeaturePlots showing the expression of DTL marker genes *Bst1* and *Aqp1*. Black arrow marks the cluster representing DTL cells. *Aqp1* is expressed not only in DTL cells but also in a subset of endothelial cells. FeaturePlots for *Pecam1* and *Hnf4a* mark the clusters for endothelium and PT cells, respectively. (B) FeaturePlots showing subsegments of PT cells. *Slc5a2* and *Ihh* mark S1 and S3 segments, respectively. While both *Slc5a8* and *Kap* mark S2/S3 segments, the activation of *Slc5a8* appears to proceed prior to that of *Kap*. (C) Aqp1 marks Hnf4a+ straight tubules but it is undetectable in convoluted PT cells in the mouse embryonic kidney. Stage, E18.5; Scale Bar, 100μm.

Figure 3. Lineage tracing of PT cells using *Slc34a1eGFPCre* shows that PT cells give rise to Aqp1+ DTL cells (A) Cre-dependent activation of *Rosa26-Sun1* reporter is detectable not only in Hnf4a+ PT cells at the cortex but also in Hnf4a- cells at the medulla. (B) In the adult mouse kidney, Aqp1 is present in both PT cells and DTL cells although DTL cells exhibit stronger Aqp1 stain than PT cells. The cells with active *Rosa26-Sun1* reporter in the medulla are positive for Aqp1 but negative for Slc12a1, suggesting that those cells are indeed DTL and not TAL. Stage, 4 month; Scale Bar, 100μm.

Figure 4. Deletion of *Hnf4a* disrupts *Aqp1* expression in DTL cells. (A) *Osr2Cre*-mediated activation of *Rosa26-LacZ* reporter marks all LOH cells in the medulla. Both control and mutant kidneys have β-galactosidase+ straight tubules and a subset of those β-galactosidase+ cells are also positive for Slc12a1, suggesting that the absence of Hnf4a does not block the elongation of the LOH or the formation of Slc12a1+ TAL cells. (B) Given *Aqp1* is expressed in both DTL and a subset of the endothelium (Figure 2A), Aqp1+ cells in the control kidney

are positive for either β-galactosidase or Pecam1. In the *Hnf4a* mutant kidney, most of the Aqp1+ tubules are positive for Pecam1, suggesting that they are all endothelial cells. A few clusters of β-galactosidase+ Aqp1+ tubules are present but they remain short, suggesting that Hnf4a is required for the proper expression of *Aqp1* in DTL cells. Stage, P10; Scale Bar, 100μm.

Figure 1

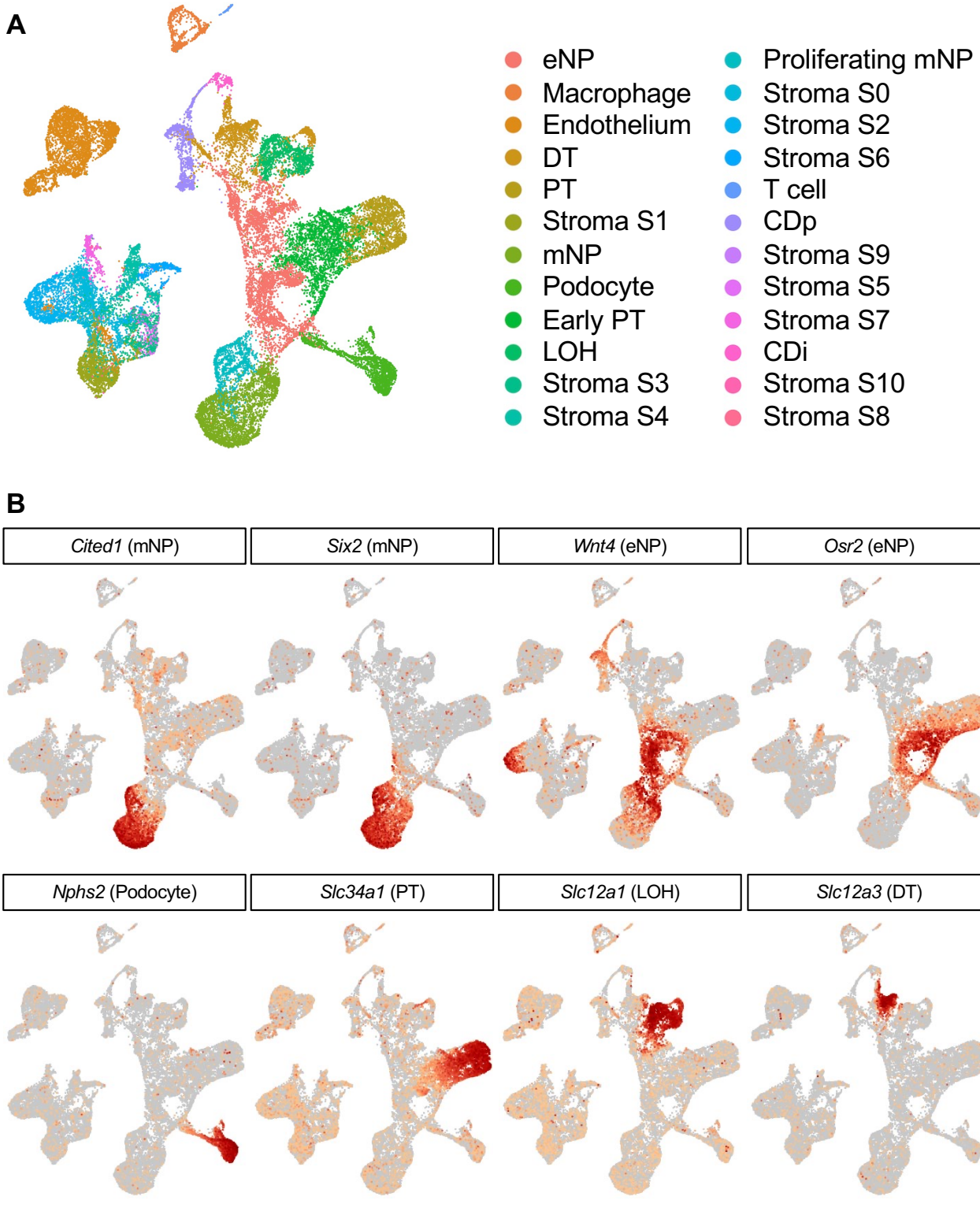

Figure 2

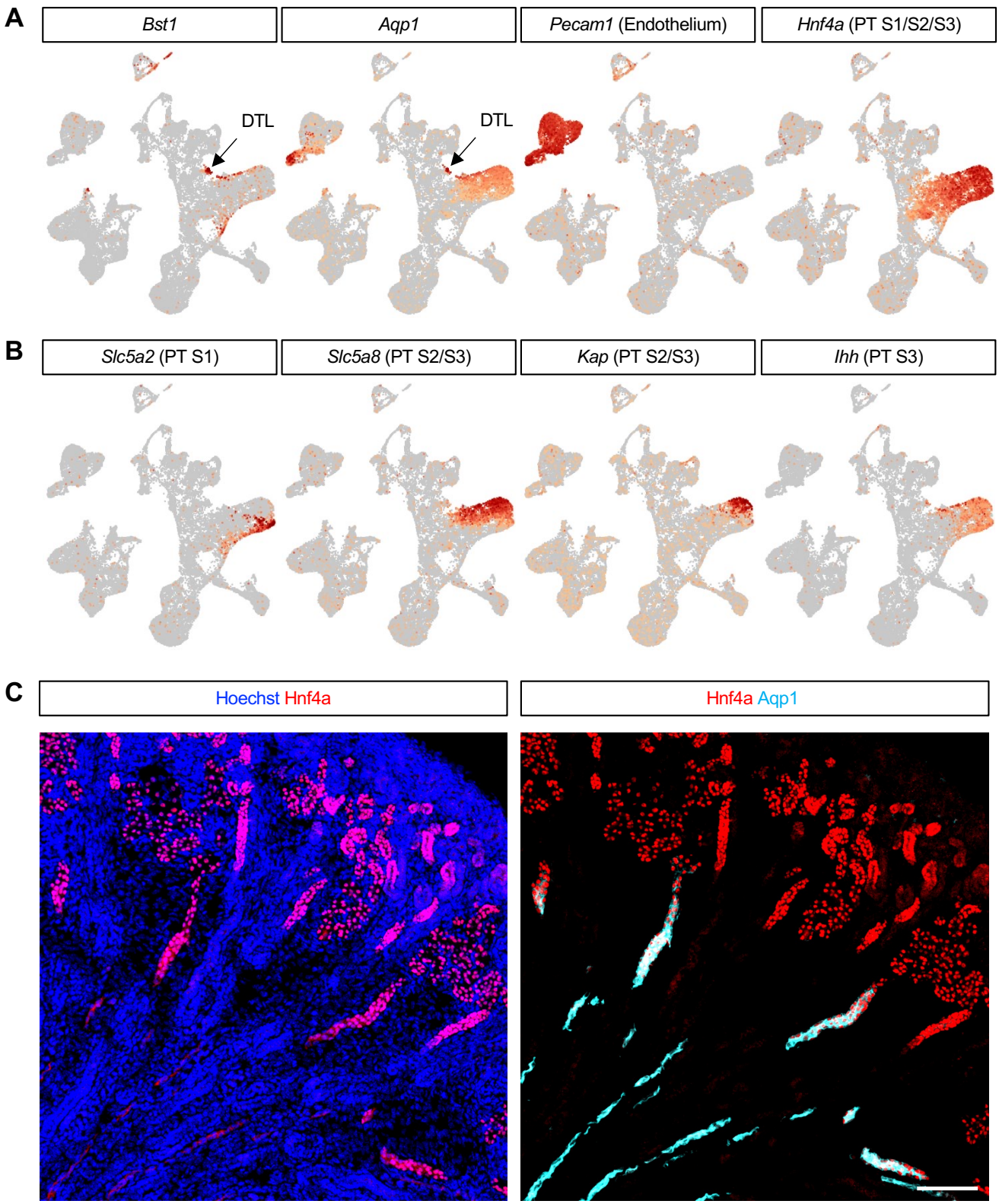

Figure 3

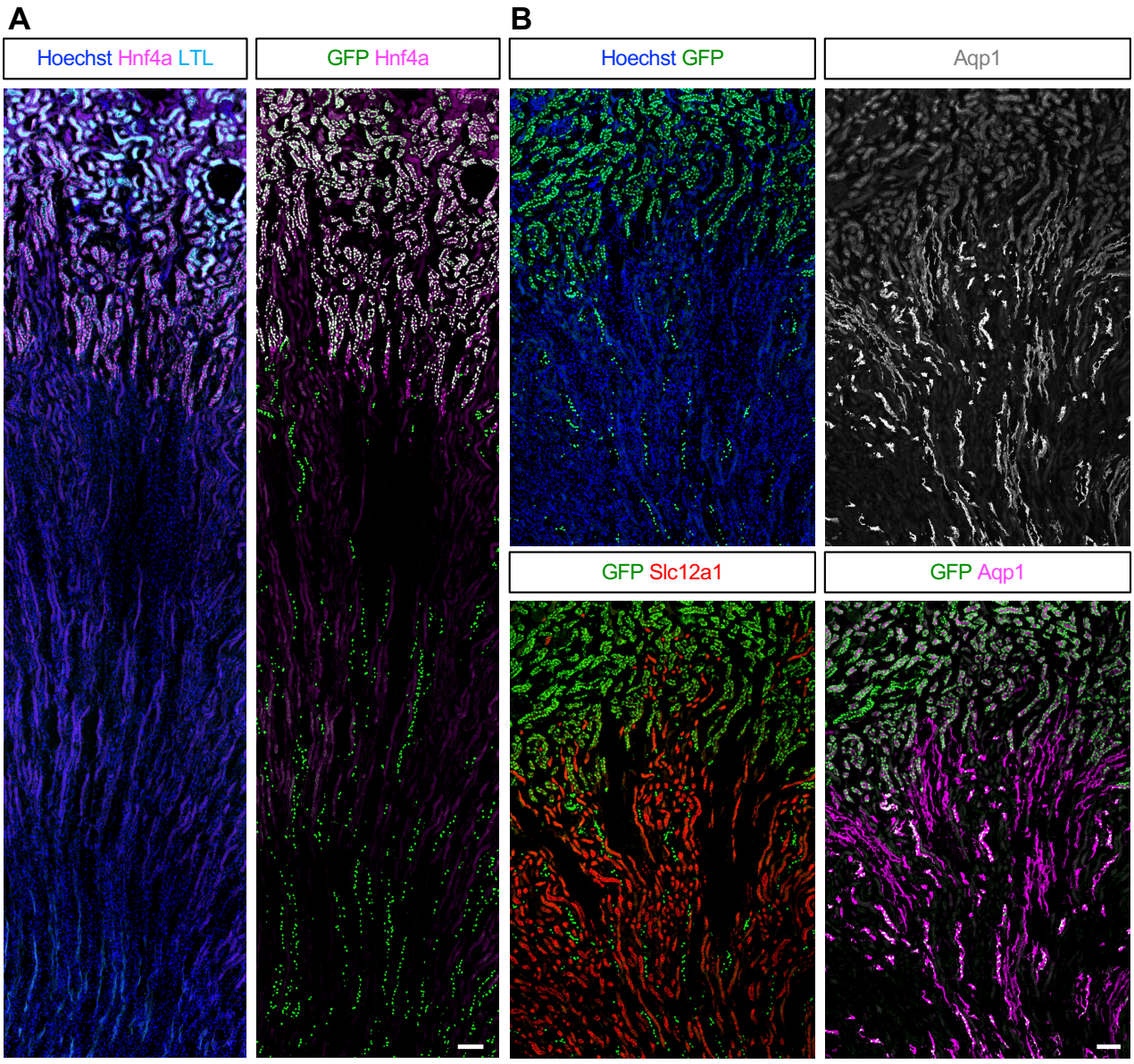

Figure 4